

Electric-field enhancement of beam coupling in $\text{Sn}_2\text{P}_2\text{S}_6$

A. Shumelyuk¹, S. Odoulov¹, D. Kip^{2,*}, E. Krätzig²

¹Institute of Physics, National Academy of Sciences, 03650, Kiev-39, Ukraine
(Fax: +380-44/265-2359, E-mail: shumeluk@iop.kiev.ua)

²Fachbereich Physik, Universität Osnabrück, Barbarastrasse 7, 49069 Osnabrück, Germany
(Fax: +49-541/969-3510)

Received: 25 October 2000 / Revised version: 18 January 2001 / Published online: 21 March 2001 – © Springer-Verlag 2001

Abstract. The influence of an external field on photorefractive recording in $\text{Sn}_2\text{P}_2\text{S}_6$ (SPS) crystals is studied. A large gain factor of more than 15 cm^{-1} is achieved for a grating spacing of $12\text{ }\mu\text{m}$ at $\lambda = 0.9\text{ }\mu\text{m}$. For an applied field exceeding $\pm 200\text{ V/cm}$ a switching of the beam coupling direction is detected, exhibiting a pronounced hysteresis.

PACS: 42.65.Hw; 42.70.Nq

Tin hypophosphite ($\text{Sn}_2\text{P}_2\text{S}_6$, SPS) [1] attracts attention because of a fast response and a wide range of spectral sensitivity ($0.5\text{--}1.3\text{ }\mu\text{m}$ [2]), though the gain factor decreases for longer wavelengths. The application of a dc electric field to photorefractive crystals results, to a first approximation, in the recording of a phase grating that coincides with the light fringes. This leads to the enhancement of the grating's diffraction efficiency but does not affect the beam coupling. Only a field that is comparable to the so-called limiting space-charge field, $E_q = (eN_A/2\pi\epsilon\epsilon_0)\Lambda$ (with e being the electron charge, N_A the effective trap density, $\epsilon\epsilon_0$ the dielectric constant, and Λ the fringe spacing), may enhance the beam coupling and increase the gain factor [3]. In practice such an enhancement occurs for nominally undoped crystals with trap-density limitations of the space-charge field, such as different crystals of the sillenite family [4].

The purpose of this paper is to check the possibility of an improvement in the beam coupling in nominally undoped SPS. With this in mind, we evaluate at first the necessary crystal parameters from experiments with no field applied, define the optimum spatial frequencies at which the enhancement can be expected, and finally demonstrate a considerable increase (about three times) in the gain factor with cw near-infrared laser radiation.

1 Experimental technique

A sketch of the experimental set-up is shown in Fig. 1. The 10-times expanded laser beam from a Ti:sapphire laser is split into two beams by a semi-transparent mirror M_2 . A stronger beam sent to the sample by a mirror M_4 illuminates the whole input face of the sample. This prevents the formation of a large-scale space-charge field in the experiments because of the applied field, and at the same time it ensures the same interaction length (equal to sample thickness) for all of the crossing angles of the recording beams that were used. To form a probe beam of smaller diameter, the other beam, reflected by the mirror M_3 , is directed to the aperture D_1 . The beam intensity ratio is 1 : 600, i.e., the light modulation is $m \simeq 0.08$. The second aperture D_2 in front of the detector PD allows only the transmitted probe beam to pass and prevents

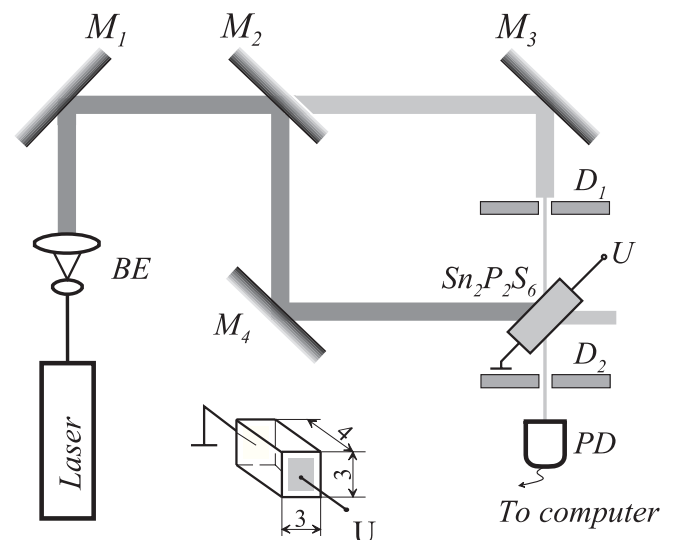


Fig. 1. Schematic of the experimental set-up. M: mirrors; D: apertures; PD: photodiode; BE: beam expander. The dimensions of the sample are given in mm

*Corresponding author.

the detection of scattered light. The signal of the detector is fed to a computer.

An *c*-cut, $4 \times 3 \times 3 \text{ mm}^3$ sample (spontaneous polarization axis P_s lies within 10° along the longest dimension) is used for beam-coupling experiments. Silver electrodes are deposited to the *a*-faces of the sample. The SPS crystal was grown, poled and optically finished at the Institute of Solid State Physics and Chemistry, Uzhgorod State University (Ukraine).

The light beam of the Ti:sapphire laser (TEM_{00} , $\lambda = 0.9 \mu\text{m}$) is linearly polarized in the plane of incidence. This optimizes the gain factor for the grating vector parallel to the OX crystallographic axis (almost parallel to the spontaneous polarization axis [5]). A dc external field is applied along the grating vector.

It has been found previously [2] that all photorefractive SPS crystals available to us (more than a dozen samples tested) can be divided into two groups, Type I and Type II, thus distinguishing the samples by the beam-coupling dynamics and spectral sensitivity of their photorefractive response. We have recently found experimentally that higher fields, at least up to 2 kV/cm , can be applied to Type II samples (less sensitive in the infrared), as compared to Type I samples. While the reason for such a difference is not completely clear at present, it seems that the reduced dark and photo-conductivities ensure a higher breakdown voltage for Type II crystals. A 2 kV/cm external field is comparable to the diffusion field for a grating spacing $\Lambda = 1 \mu\text{m}$ ($E_D = 1.6 \text{ kV/cm}$), so it might be sufficient for an increase in the gain factor of up to two times.

The gain factor Γ is determined in the usual way from

$$\Gamma = \frac{1}{\ell} \ln \frac{I_s(\ell)}{I_s(0)}, \quad (1)$$

where $I_s(\ell)$ and $I_s(0)$ are the intensities of the weak transmitted beam in the presence of a strong pump beam and without a pump beam, respectively, and ℓ is the sample thickness. For the sample K1 (Type II) the out-of-phase compensating grating [1] is negligibly small, so the steady-state intensity of the transmitted probe beam can be taken to evaluate Γ .

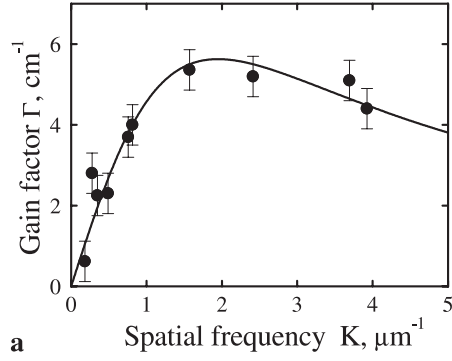
The following sequence is applied to the sample when measuring the gain factor: first the electric field, then the strong pump beam, and last the weak probe beam.

We also measured the relaxation time, τ , of the refractive-index change from the dynamics of the signal decay when the input probe beam is switched off after saturation is reached.

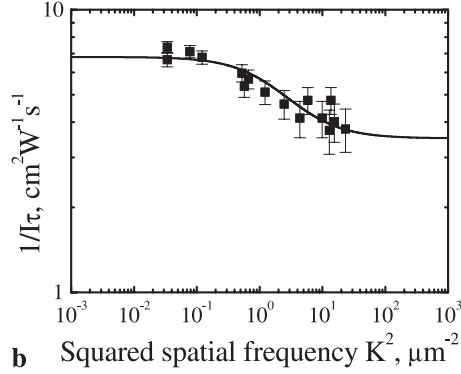
2 Sample characterization

The spatial-frequency dependence of the gain factor Γ is shown in Fig. 2a, while Fig. 2b presents the spatial-frequency dependence of the reciprocal decay time normalized to the total light intensity in the sample, $(\tau I)^{-1}$. No external field is applied to the sample in this experiment. The two dependences shown in Fig. 2 allow for the evaluation of the Debye screening length,

$$\ell_s = \sqrt{\frac{\varepsilon \varepsilon_0 k_B T}{e^2 N_A}}; \quad (2)$$



a



b

Fig. 2. **a** Spatial-frequency dependence of gain factor and **b** normalized reciprocal relaxation time versus squared spatial frequency. *Solid lines:* best fit of the theoretical dependences (5) and (6), respectively

the diffusion length,

$$\ell_D = \sqrt{D\tau_c}; \quad (3)$$

the dielectric relaxation time (Maxwell relaxation time),

$$\tau_{\text{di}} = \frac{\varepsilon \varepsilon_0}{\sigma}; \quad (4)$$

and the effective electro-optic constant, r_{eff} . All these crystal parameters can be obtained from a fit of the theoretical dependences [3, 4] to the experimental data:

$$\Gamma = \frac{2\pi r_{\text{eff}} n^3}{\lambda} E_{\text{sc}} = \frac{2\pi r_{\text{eff}} n^3}{\lambda} \frac{k_B T}{e} \frac{K}{1 + K^2 \ell_s^2}, \quad (5)$$

$$\frac{1}{\tau_i I_0} = \frac{1}{\tau_{\text{di}} I_0} \frac{1 + K^2 \ell_s^2}{1 + K^2 \ell_D^2}, \quad (6)$$

Here k_B is the Boltzmann constant, T is the absolute temperature, $D = \mu k_B T / e$ is the diffusivity, μ is the charge mobility, τ_c is the charge lifetime, λ is the light wavelength in vacuum, $\sigma = \kappa I_0$ is the photoconductivity, κ is the specific photoconductivity, and $K = 2\pi/\Lambda$ is the grating spatial frequency.

The following data were obtained from the fit: $\ell_s \approx 0.5 \mu\text{m}$, $\ell_D \approx 0.7 \mu\text{m}$, $r_{\text{eff}} \approx 130 \text{ pm/V}$, $\kappa \approx 1.4 \times 10^{-10} \text{ cm/V}^2$. The effective trap density evaluated by using (2) is $N_A \approx 1.3 \times 10^{15} \text{ cm}^{-3}$, providing that the dielectric constant is $\varepsilon = 230$. The limiting space charge field in V/cm is therefore $E_q \approx 160 \times \Lambda$, with Λ measured in microns. It is obvious that for spatial frequencies of the grating $\Lambda = 1\text{--}10 \mu\text{m}$ typical for our experimental conditions the value of the limiting space-charge field is quite reasonable, $E_q = 160\text{--}1600 \text{ V/cm}$.

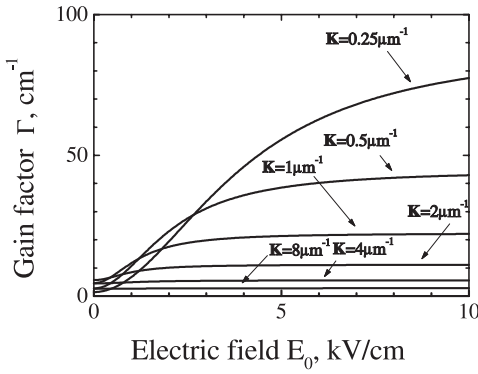


Fig. 3. Calculated dependency of the gain factor versus applied field for different spatial frequencies of the recorded grating

With the evaluated data we can predict the behavior of beam coupling in the sample with an applied field. To do so we need to substitute E_{sc} in (5) with the expression describing the imaginary part of the space-charge field developing with the applied field [3, 4]:

$$\text{Im}\{E_{sc}\} = \frac{E_D(1 + K^2\ell_s^2) + \ell_E K E_0}{(1 + K^2\ell_s^2)^2 + (K\ell_E)^2}, \quad (7)$$

$\ell_E = \varepsilon\varepsilon_0 E_0 / eN_A$ being the tightening length of the charge by the electric field [3].

Figure 3 shows the calculated electric-field dependence of the gain factor for different values of the spatial frequency K . One can see that for small grating spacings (large values of K) the gain factor is nearly independent of the applied field within the plotted range of E_0 . It is obvious that to reach the highest possible gain factor one should go to spatial frequencies much smaller than those that optimize the gain with no field applied.

3 Experiments with an applied field

In accordance with the conclusions of Sect. 2, a spatial frequency $K \approx 0.5 \mu\text{m}^{-1}$ ($\Lambda = 12 \mu\text{m}$) was chosen for the grating recording with an applied field. The electric-field dependence of the gain factor is shown in Fig. 4. The solid line represents the dependence calculated from (5) and (7) with the parameters evaluated in Sect. 2. One can see a qualitative agreement between the experimental and calculated data, but with a 30% reduction of the gain factor as compared with that expected from the calculation. This discrepancy is most probably related to the formation of a large-scale space-charge field in the sample, which is due to imperfect homogeneous illumination. In other words, the real field in the highly illuminated region of the crystal is smaller than the applied field.

Figure 5 shows the spatial frequency dependence of the gain factor with $E_0 = 2 \text{ kV/cm}$ (solid dots). For comparison, the experimental data with no field applied are also shown (open squares). The solid and dashed lines give the dependences calculated from (5) and (7).

One can see from the data in Fig. 5 that the application of an external field strongly enhances the gain. Not only is the gain factor with an external field larger than the initial

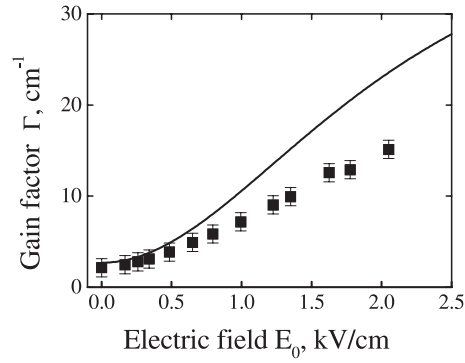


Fig. 4. Gain factor versus applied field. Dots: measured values; solid line: expected theoretical dependence for $K = 0.5 \mu\text{m}^{-1}$

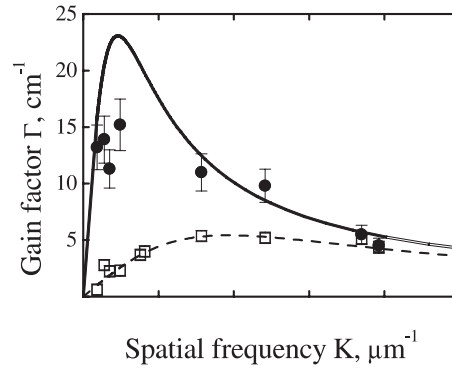


Fig. 5. Spatial frequency dependence of the gain factor with an applied field of 2 kV/cm (solid dots) and with no field (open squares). Dashed line: fit of (5); solid line: obtained from (5) and (7) with the set of parameters extracted from the fit of the data with no field

gain factor at the same spatial frequency (where it is not optimized), but it becomes nearly three times larger than its optimum value with no field. With the largest gain factor, the signal beam is amplified 100 times.

An even higher gain might be expected for larger applied fields (the calculated dependences of the gain factor for $K = 0.5$ and 0.25 are obviously not saturated at $E_0 = 2.5 \text{ kV/cm}$, see Fig. 3). In practice we are limited, however, by the threshold of electrical breakdown, which is not much larger than 2 kV/cm for the available samples.

It should be emphasized that only the dashed line in Fig. 5 is the best fit to (5); the solid line is calculated with parameters extracted from (5) and (7) and the set of parameters extracted from the fit of the data with no field. In spite of a quite large scattering of the experimental data with the applied field as compared to $E_0 = 0$, a reasonable qualitative agreement with the calculation can be seen. Apart from the gain enhancement, we clearly observe a shift of the gain factor maximum towards smaller spatial frequencies with the electric field applied, as predicted by (5) and (7). Qualitatively, this shift can be explained by a spatial-frequency dependence of the limiting space-charge field.

Until now only the data for the field applied along the spontaneous polarization direction were shown. When the polarity of the applied field is reversed, we observe a switching of the beam-coupling direction. Fig. 6 shows this behavior for an applied field gradually changing from -2 kV/cm to $+2 \text{ kV/cm}$ for a grating with spatial frequency $K \approx 3 \mu\text{m}^{-1}$

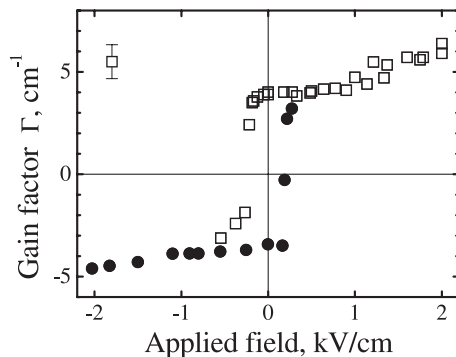


Fig. 6. Gain factor versus applied field with changing polarity. The grating spatial frequency is $K = 3 \mu\text{m}^{-1}$

($\Lambda = 2 \mu\text{m}$). The applied electric field was changed step by step, either increased or decreased, when measuring the dependence shown in Fig. 6. It was never dropped down to zero between two consecutive measurements.

A pronounced hysteresis is observed with a coercive field of about 200 V/cm . An electric-field-controlled beam-coupling direction and hysteresis have already been reported for SBN and SPS crystals [5–7]. It is supposed that a ferroelectric P – E hysteresis (spontaneous polarization versus applied electric field) is the origin of the hysteresis behavior in the gain factor versus applied field. The switching of the beam-coupling direction to the opposite one is attributed to a spontaneous-polarization reversal under the coercive field E_c [6].

The coercive field ranged within an interval from 1 to 2 kV/cm for SBN [5, 6], and from 0.6 to 1 kV/cm for SPS crystals [7], i.e., it is larger than or comparable to the diffusion field ($k_B T/e$) K during grating recording. We show for SPS crystals of Type II that the coercive field can be considerably smaller ($\approx 200 \text{ V/cm}$) than the diffusion field ($\approx 800 \text{ V/cm}$). This might lead to the formation of a regular domain structure with a periodically inverted spontaneous polarization in the case of a high contrast of the recording light fringes. In our experiment the domain reversal does not occur during grating recording because the space charge field that self-develops in the sample ($E_{sc} = m E_D$) is considerably reduced because of the small light modulation, $m \approx 0.08$.

A small grating spacing $\Lambda \approx 2 \mu\text{m}$ is selected in this particular experiment to emphasize the difference in the coercive field and the diffusion field. Nevertheless, a 1.5-times enhancement of the gain factor is reached with an applied field of 2 kV/cm , even with this unfavorable spatial frequency.

4 Conclusions

We have shown that at least a three-times enhancement of the gain factor can be achieved by applying a moderate dc electric field to an $\text{Sn}_2\text{P}_2\text{S}_6$ sample during photorefractive grating recording. It is important to mention that even with the applied field the response time remains in the millisecond range at an intensity of about 20 W/cm^2 of the Ti:sapphire laser radiation at $\lambda = 0.9 \mu\text{m}$.

Hysteresis is observed in the beam-coupling direction that can be reversed by the application of an electric field exceeding the coercive field of 200 V/cm . The field-controlled direction of the beam coupling remains the same after switching off the field, as was reported previously for SBN crystals [6]; however, a reduced gain factor is incurred.

Acknowledgements. Financial support of the Deutsche Forschungsgemeinschaft (grant SFB 225, A6) is gratefully acknowledged. We would like to thank A. Grabar and I. Stoyka for the SPS sample used in the present study and our reviewers for constructive criticism and valuable suggestions.

References

1. S. Odoulov, A. Shumelyuk, U. Hellwig, R. Rupp, A. Grabar: *J. Opt. Soc. Am. B* **13**, 2352 (1996)
2. A. Shumelyuk, S. Odoulov, Yi Hu, E. Kraetzig, G. Brost: *CLEO '98 Technical Digest*, San Francisco (1998) pp. 171–172
3. N. Kukhtarev, V. Markov, S. Odoulov, M. Soskin, V. Vinetskii: *Ferroelectrics* **22**, 946,961 (1979)
4. S.I. Stepanov, M.P. Petrov: In *Photorefractive materials and their applications*, TAP 61 (Springer, Berlin, Heidelberg 1988) pp. 263–289
5. A.V. Knyaz'kov, N.M. Kozhevnikov, Y.S. Kuz'minov, N.M. Polozkov, A.S. Saikin, S.A. Sergushenko: *Sov. Technol. Phys. Lett.* **9**, 123 (1983)
6. T. Woike, T. Wolk, U. Dorfler, R. Pankrath, L. Ivleva, M. Wöhlecke: *Ferroelectr. Lett.* **23**, 127 (1998)
7. A. Grabar, R. Muzhikash, A. Kostyuk, Y. Vysochanski: *Sov. Phys. Solid State* **33**, 1314 (1991)